ISBN: 978-3-95450-227-1 ISSN: 2673-5490 doi:10.18429/JACoW-IPAC2022-WEPOTK064

GENERATING SUB-FEMTOSECOND ELECTRON BEAMS AT PLASMA WAKEFIELD ACCELERATORS

R. R. Robles*, C. Emma, R. Hessami, K. Larsen, A. Marinelli,
SLAC National Acccelerator Laboratory, CA, USA

Abstract

The Plasma-driven Attosecond X-ray source (PAX) project at FACET-II aims to produce attosecond EUV/soft x-ray pulses with milijoule-scale pulse energy via nearly coherent emission from pre-bunched electron beams. In the baseline approach [1, 2], a beam is generated using the density downramp injection scheme with a percent-per-micron chirp and 10^{-4} scale slice energy spread. Subsequent compression yields a current spike of just 100 as duration which can emit 10 nm light nearly coherently due to its strong pre-bunching. In this work, we report simulation studies of a scheme to generate similarly short beams without relying on plasma injection. Instead, we utilize a high-charge beam generated at an RF photocathode, with its tail acting as the witness bunch for the wake. The witness develops a percent-per-micron chirp in the plasma which is then compressible downstream. The final bunch length demonstrated here is as short as 100 nm, and is limited primarily by emittance effects. The configurations studied in this work are available for experimental testing at existing PWFA facilities such as FACET-II.

INTRODUCTION

There is significant recent interest in attosecond science due to the realization of attosecond x-ray pulse generation with high pulse energy at x-ray free-electron lasers (XFELs) [3]. Typical performance in this case for soft x-ray wavelengths is typically tens of microjoules per pulse and several hundred attosecond pulse durations. To push the pulse energy higher and the pulse duration shorter while still utilizing the relatively high efficiency of the FEL process, one requires higher electron beam brightness. It was proposed in [1] to take advantage of the high-quality beams projected to be generated by plasma wakefield accelerators to achieve this goal. This scheme is called the Plasma-driven Attosecond X-ray source (PAX). PAX combines two key concepts to generate mega-ampere class, sub-femtosecond electron beams. The first is the production of an initial beam with very low emittance and energy spread from advanced wakefield injection techniques - in this case, density downramp injection [4]. The plasma injected beam can naturally be produced with very high linear energy chirp on the order of a few %/μm due to the sawtooth nature of nonlinear plasma wakes. Such high chirps, when compressed in a magnetic chicane, lead to very short beams with minimal length limited to $R_{56}\sigma_\gamma$ where R_{56} is the momentum compaction of the chicane and σ_γ is slice energy spread of the original beam. In reality, chromatic and collective effects can conspire to limit the final pulse length to values larger than this minimum.

One of the key prerequisites of the PAX project as outlined in [1] is the demonstration of density downramp injection to achieve the high beam brightness. Before density downramp injection is available at FACET-II, it was also suggested that one could achieve a similar final beam profile by accelerating drive and witness bunches generated by an RF photoinjector together to produce a strongly chirped beam. In the present work we present yet another mechanism, in which a single bunch is accelerated through a standard RF accelerator such that it enters the plasma with a long tail. The tail then experiences the wake of the core of the bunch the same way as a separately generated witness bunch, and can similarly be compressed to ultrashort duration thereafter. We present simulation results based on the FACET-II facility indicating performance fitting for a stepping stone towards the plasma injected case [5].

BEAMLINE OVERVIEW

The simulation results presented below were all obtained using the Lucretia code [6]. The FACET-II beamline consists of a conventional RF photoinjector which injects the beam into the primary linac at roughly 135 MeV. From there the beam goes through three linac sections, L1, L2, and L3, arriving at the final energy 10 GeV. Between L1/L2 and L2/L3 there are four-dipole chicanes, BC11 and BC14, which facilitate compression of the beam. Finally, at the end of L3 immediately preceding the plasma portion of the beamline is a third bunch compressor, BC20, which employs a complicated set of optics to achieve anomalous compression.

The FACET-II injector can operate in single and dual bunch mode. In the present work we focus on the single bunch configuration, launching a 2 nC beam from the cathode with a 4 ps laser pulse length. The quality of the resulting beam is summarized in Fig. 1, as simulated in General Particle Tracer (GPT) [7].

From then on the beamline is optimized to achieve the highest possible peak current at the end of BC20. The longitudinal phase spaces and current profiles are shown after each bunch compressor in Fig. 2. By the time the beam has been compressed in BC14 there is a clear third-order curvature, which after subsequent acceleration and compression in BC20 transforms the beam into a highly nonlinear S-shaped longitudinal phase space. On either side of the >100 kA core are long regions of the beam with roughly flat phase space, low slice energy spread, and currents still largely exceeding 1 kA.

* riverr@stanford.edu

ISBN: 978-3-95450-227-1 ISSN: 2673-5490 doi:10.18429/JACoW-IPAC2022-WEPOTK064

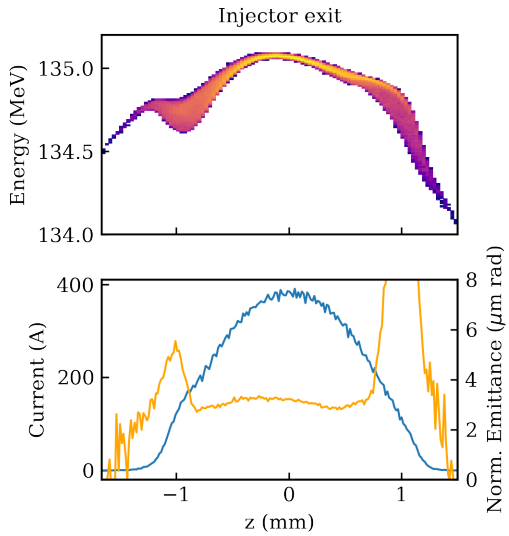

Figure 1: The longitudinal phase space (top) and slice current and emittance (bottom) of the beam at the exit of the injector.

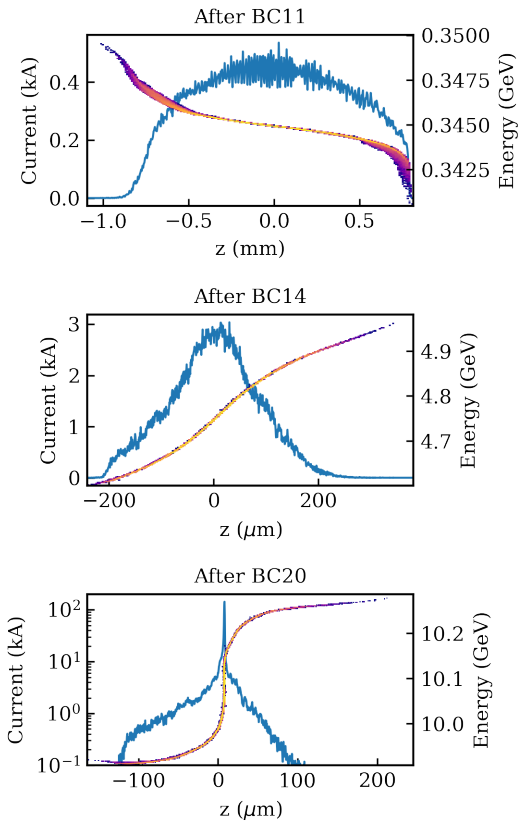

Figure 2: The longitudinal phase space and current are plotted after each of the three bunch compressors.

We further highlight the properties of the long tail in Fig. 3. Here we have plotted the current, normalized emittance, and energy spread along the bunch length. We see that within the tail the current remains above 1 kA out to about 100 μm behind the core, and the slice energy spread is roughly 0.5 MeV uniformly. The normalized slice emittance is well-preserved up to 25 μm behind the core before beginning to grow to > 10 μm further beyond that.

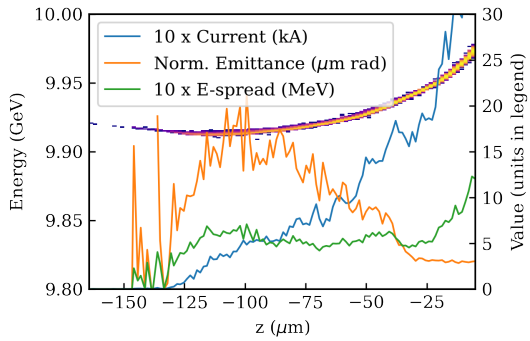

Figure 3: The longitudinal phase space of the tail of the bunch after BC20 is plotted along with its slice current, emittance, and energy spread.

PLASMA SECTION

Estimates for Available Sources

We with some general considerations regarding the plasma interaction in the blowout regime [8]. The plasma bubble in the blowout regime is roughly λ_p long, with $\lambda_p = 2\pi c/\omega_p$ where $\omega_p = \sqrt{e^2 n/m_e \epsilon_0}$ is the plasma frequency. Thus the location of the zero-crossing of the wake is at roughly $\lambda_p/2$ behind the bunch core. The default plasma source at FACET-II is a meter long lithium oven with achievable densities in the range $10^{16} - 10^{17}$ cm^{-3}. This would place the center of the bubble in the range 50-160 μm behind the bunch core. This places the portion of the tail which is at slightly higher emittance at the zero-crossing of the wakefield, which is not ideal but not necessarily devastating.

In addition to the oven, FACET-II also supports a gas jet with densities as high as $5 \times 10^{18} - 10^{20}$ cm^{-3} [9]. This places the wakefield zero crossing as close as a few microns from the drive bunch. This would enable us to access the higher current, lower emittance portion of the tail. The gas jet itself would only produce a 5 mm long plasma, but with the much higher densities the expected chirp is still large.

The wakefield in the bubble is roughly linear with a gradient given approximately by $E_z' \simeq m\omega_p^2/2e$. Thus the relative chirp for central energy 10 GeV is in the range $0.9 - 9\%/\mu$m for the oven and $2.3 - 45\%/\mu$m for the gas jet. These chirps are on the same order as that obtained in [1], with similarly comparable slice energy spread.

Semi-analytic Tracking

In lieu of full PIC simulations, we have implemented the equations in [10], since for the low current tail beam loading effects should be negligible. We begin by simulating the dynamics of the tail through a 5 mm long plasma

ISBN: 978-3-95450-227-1 ISSN: 2673-5490 doi:10.18429/JACoW-IPAC2022-WEPOTK064

with a super-gaussian plasma density profile with peak value 5×10^{18} cm^{-3}. The characteristics of the tail of the beam following the plasma section are outlined in Fig. 4. Comparing it to Fig. 3, we note that aside from the strong linear chirp imposed on the longitudinal phase space, the slice-wise qualities of the beam can be roughly preserved so long as the beam is properly matched transversely into the plasma. The linear chirp is roughly 0.26 GV/μm.

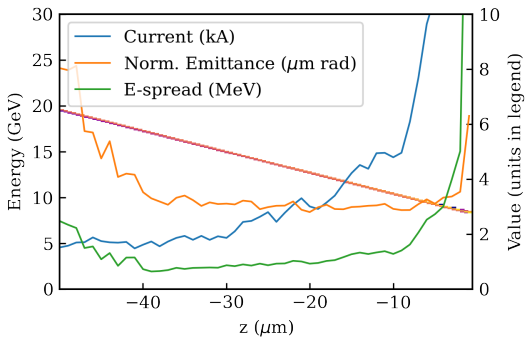

Figure 4: The longitudinal phase space of the tail of the bunch after the gas jet plasma is plotted along with its slice current, emittance, and energy spread.

Compressing this chirp has some limitations, however, in particular from the impact of emittance-induced debunching which results from the reduction of axial velocity due to transverse angles: $\beta_z = \sqrt{1 - \frac{1}{\gamma^2} - (x')^2 - (y')^2}$. In the FACET-II beamline the beam will have to propagate several meters between the end of the gas jet and the compressing chicane. This fact, coupled with the very small matched beam size in the high density plasma, causes substantial debunching from emittance. Attempts to mitigate this effect are in progress.

These effects are slightly less exaggerated for the lithium oven plasma source due to the shorter distance between it and the chicane, as well as the larger matched beam size in the plasma. This is the case in spite of the larger emittance in the portion of the beam left at 10 GeV in the lithium oven. In this case due the longer plasma, the emittance debunching effects are stronger during acceleration, as seen in Fig. 5.

The behavior of the quadrupole triplet and compressor is modelled in *elegant* [11], and is summarized for the lithium oven in Fig. 6. We note that the compression is highly non-linear, but still yields a > 40 kA spike of roughly 100 nm full-width at half-maximum. Furthermore, slice emittance reduction is observed in the current spike as a result of emittance debunching preferentially delaying high-divergence particles.

CONCLUSIONS AND OUTLOOK

We have presented preliminary simulation studies implementing the PAX concept with a single bunch generated by an RF photocathode by treating the tail of the bunch as an effective witness beam. Due to the naturally low energy spread found in the bunch tail and its proximity to the core, it can be given a very large chirp in the plasma which can subsequently be compressed to a very short, sub-femtosecond current spike. These results provide benchmark goals for the large PAX project on the way to the ultimate realization in the style of [1].

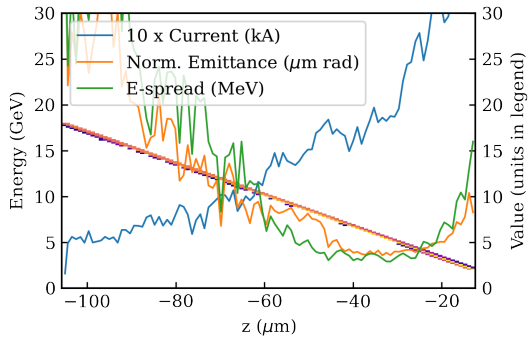

Figure 5: The longitudinal phase space of the tail of the bunch after the lithium oven plasma is plotted along with its slice current, emittance, and energy spread.

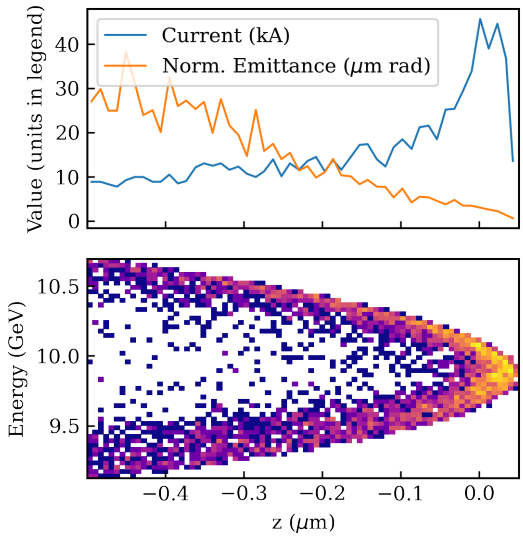

Figure 6: The longitudinal phase space (bottom) and slice properties (top) of the beam accelerated in the lithium oven plasma is shown after compression in a magnetic chicane.

ACKNOWLEDGEMENTS

This work was supported by the Department of Energy, Laboratory Directed Research and Development program at SLAC National Accelerator Laboratory, under contract DE-AC02- 76SF00515. This work was also partially supported by the DOE under Grant No. DE-SC0009914. R.R.R. acknowledges the support of the William R. Hewlett fellowship through the Stanford Graduate Fellowship program.

ISBN: 978-3-95450-227-1 ISSN: 2673-5490 doi:10.18429/JACoW-IPAC2022-WEPOTK064

REFERENCES

[1] C. Emma *et al.*, "Terawatt attosecond x-ray source driven by a plasma accelerator," *APL Photonics*, vol. 6, no. 7, p. 076 107, 2021.

[2] C. Emma *et al.*, "PAX: A Plasma-Driven Attosecond X-Ray Source," in *Proc. IPAC'21*, Campinas, Brazil, May 2021, pp. 2755–2758, doi:10.18429/JACoW-IPAC2021-WEPAB072

[3] J. Duris *et al.*, "Tunable isolated attosecond x-ray pulses with gigawatt peak power from a free-electron laser," *Nature Photonics*, vol. 14, no. 1, pp. 30–36, 2020.

[4] X. Xu *et al.*, "High quality electron bunch generation using a longitudinal density-tailored plasma-based accelerator in the three-dimensional blowout regime," *Physical Review Accelerators and Beams*, vol. 20, no. 11, p. 111 303, 2017.

[5] V. Yakimenko *et al.*, "Facet-ii facility for advanced accelerator experimental tests," *Physical Review Accelerators and Beams*, vol. 22, no. 10, p. 101 301, 2019.

[6] P. Tenenbaum, "Lucretia: A Matlab-Based Toolbox for the Modeling and Simulation of Single-Pass Electron Beam Transport Systems," in *Proc. PAC'05*, Knoxville, TN, USA, May 2005, pp. 4197–4199, doi:10.18429/JACoW-PAC05-FPAT086

[7] M. De Loos and S. Van der Geer, "General particle tracer: A new 3d code for accelerator and beamline design," in *5th European Particle Accelerator Conference*, 1996, p. 1241.

[8] W. Lu, C. Huang, M. Zhou, W. Mori, and T. Katsouleas, "Nonlinear theory for relativistic plasma wakefields in the blowout regime," *Physical review letters*, vol. 96, no. 16, p. 165 002, 2006.

[9] S. Corde, K. Marsh, and F. Fiuza, "E-305: Beam filamentation and bright gamma-ray bursts," in *FACET-II Science Workshop 2019*, 2019.

[10] R. Ariniello, C. Doss, V. Lee, C. Hansel, J. Cary, and M. Litos, "Chromatic dynamics of an electron beam in a plasma based accelerator," 2021, doi:10.48550/arXiv.2111.02332

[11] M. Borland, "Elegant: A flexible sdds-compliant code for accelerator simulation," Argonne National Lab., IL, USA, Tech. Rep., 2000.